

PRISM-0: A Predicate-Rich Scene Graph Generation Framework for Zero-Shot Open-Vocabulary Tasks

Abdelrahman Elskhawy^{1,2} Mengze Li^{1,2} Nassir Navab¹ Benjamin Busam¹

¹Technical University of Munich

²Zeiss Meditec AG

Abstract

In Scene Graphs Generation (SGG) one extracts structured representation from visual inputs in the form of objects nodes and predicates connecting them. This facilitates image-based understanding and reasoning for various downstream tasks. Although fully supervised SGG approaches showed steady performance improvements, they suffer from a severe training bias. This is caused by the availability of only small subsets of curated data and exhibits long-tail predicate distribution issues with a lack of predicate diversity adversely affecting downstream tasks. To overcome this, we introduce PRISM-0, a framework for zero-shot open-vocabulary SGG that bootstraps foundation models in a bottom-up approach to capture the whole spectrum of diverse, open-vocabulary predicate prediction. Detected object pairs are filtered and passed to a Vision Language Model (VLM) that generates descriptive captions. These are used to prompt an LLM to generate fine-and-coarse-grained predicates for the pair. The predicates are then validated using a VQA model to provide a final SGG. With the modular and dataset-independent PRISM-0, we can enrich existing SG datasets such as Visual Genome (VG). Experiments illustrate that PRISM-0 generates semantically meaningful graphs that improve downstream tasks such as Image Captioning and Sentence-to-Graph Retrieval with a performance on par to the best fully supervised methods.

1. Introduction

Scene Graph Generation (SGG) aims at predicting the pairwise relations between objects in a visual scene. They can provide a structured and semantically rich representation of visual input. Graph nodes thereby represent localized objects and edges constitute pairwise relationships. Scene graphs have proven crucial to visual scene understanding, improving visual reasoning capabilities and facilitating a variety of downstream tasks [7, 11] such as im-

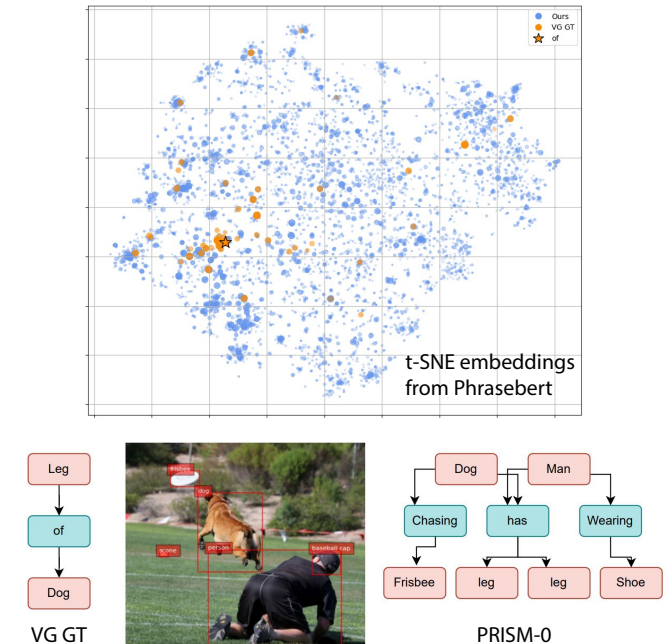


Figure 1. **Predicate Distribution for VG Labels and PRISM-0.** Top: Comparing predicate features embeddings for Visual Genome (VG) labels (orange) reveals clustering amongst a subset of predicates such as the term "of" (star). PRISM-0 predicates (blue) populate the space more densely. Bottom: An example image shows that VG labels (left) are factually correct. However, they fail to describe the semantics of the scene (middle). Our predictions, on the other hand, successfully capture both semantic and factual scene information.

age captioning [47, 48, 58], Visual Question Answering (VQA) [22], image generation [8, 14], and 3D Scene generation [9, 52, 53].

The advent of large-scale datasets, such as Visual Genome (VG) [21], has significantly propelled the field of supervised SGG by providing a large set of annotated images for training. The scale of VG and its labels in-

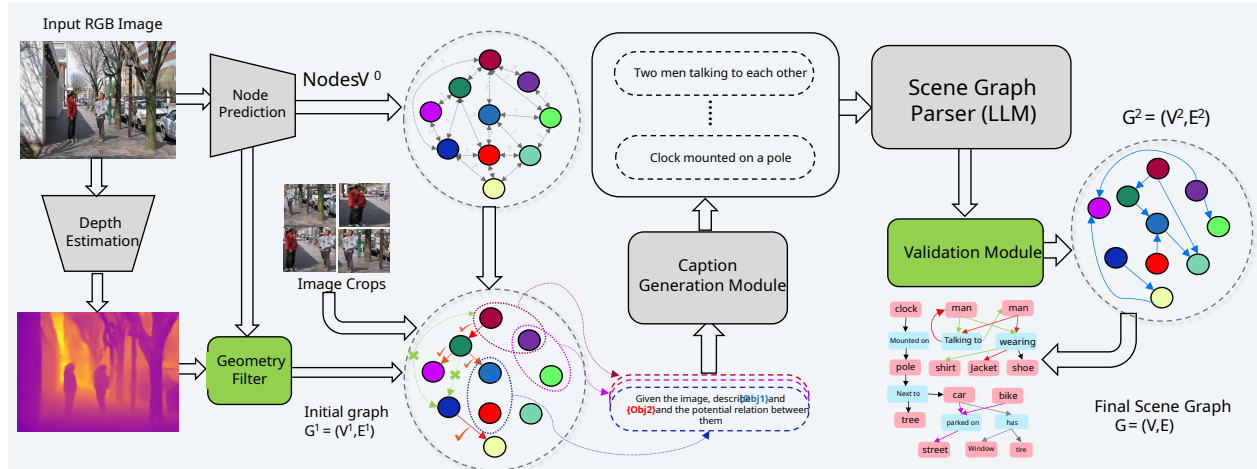


Figure 2. **Overview of the PRISM-0 framework.** The pipeline begins with node prediction and extraction of scene geometry. Pairwise captions are generated using a VLM and scene graph parsing is done with an LLM. The proposed geometric refines the relational pairs before triplet extraction. Finally, a relation validation module ensures the semantic and spatial relevance of the extracted triplets, resulting in enriched scene graphs for downstream tasks.

spired many works and is considered the de-facto standard for evaluation of SGG. Despite this undoubtedly valuable progress, further development of SGG faces challenges primarily due to the inherent bias in VG annotation. The top 50 re-occurring predicate categories account for most of the training samples, while more specific predicates lack sufficient training data [51]. A trivial sparse graph also does not provide relevant information about the scene to reason about downstream tasks. Fig. 1 (top) visualizes the distribution difference between VG ground truth (GT) labels and our predicates for a set of 7k images of the VG dataset [21] utilizing Phrasebert [41] embeddings. Although the objects in the image are almost perfectly detected, the provided SG is trivial and uninformative. While it provides factual information, e.g. *"leg of dog"*, it fails to deliver semantically meaningful information about the content of the image such as *"dog chasing frisbee"* or *"man playing with dog"*. If a supervised SGG model is trained on such mostly trivial GT labels, it will not generate meaningful representations during inference.

To address these challenges, language-supervised SGG has gained more attention in recent years [17, 56] following the recent advancements in LLMs research. Nonetheless, such methods still depend on the available GT captions for supervision and are unable to bypass the underlying issue of biased annotation while suffering from the lack of annotation diversity.

In this paper, we propose an efficient, modular, and scalable zero-shot open-vocabulary scene graph generation framework that leverages the extensive information provided by pre-trained VLMs and LLMs. Although recent VLMs show strong captioning capabilities, they are

typically trained on image-text contrastive objectives and lack nuanced linguistic skills for generating fine-grained predicate categories. However, LLMs acquired substantial knowledge about meaningful relationships from massive text corpora during general pretraining. In this work, we carefully prompt a VLM, then parse the output using an LLM, which provides a powerful tool for generating both fine-and-coarse-grained predicates. We term our approach **PRISM-0** to symbolize that we capture the whole spectrum of predicates and control this spectrum through a bottom-up approach.

Unlike previous work [28, 51] that follow a top-down approach that relies on associated image captions or GT SG annotations, our approach generates the SG directly from images, hence overcoming the bias problem and providing both known and novel semantically meaningful open-vocabulary predicates¹ overcoming the lack of label diversity. Captioning only the original image fails to depict all potential pairwise relationships. To address this, we segment the image into patches of varying sizes prior to processing. This approach enables the VLM to extract more detailed relation information by focusing on specific, enhanced segments of the image. However, given that our framework integrates multiple large foundational models, as illustrated in Fig. 2, generating and analyzing captions for the combinatorially expanding number of object pairs in dense scenes can become computationally demanding. Our core intuition for considering all object pairs is that relying solely on overlapping bounding boxes (bboxes) is insufficient to capture relevant details about the visual input. For instance, in scenes where a *person is talking to another per-*

¹Throughout the paper, we use predicates and relations interchangeably

son or a person is watching TV, the objects' bboxes may not overlap; yet, these interactions might represent the primary relational context within the image.

To overcome this challenge, we implement a series of filtering mechanisms aimed at excluding relation pairs that are either irrelevant or semantically implausible. In particular, we use depth information in conjunction with bounding boxes to estimate a 3D center for each object via the **Geometric Filter** module, shown in Fig. 2. This approach enables us to eliminate object pairs that are spatially distant, allowing us to concentrate on relations that are contextually more meaningful. A final validation model refines the output triplets generated by the scene graph parser, filtering them based on their semantic and spatial relevance in the input image.

Our main contributions are summarized as follows:

- We propose an efficient and modular zero-shot open-vocabulary scene graph generation framework that can benefit from the continuous advancements in VLMs and LLMs.
- Our bottom-up paradigm allows the framework to consider all relation pairs in the image not just the ones with overlapping bboxes, making the generated SG richer and boosting downstream tasks performance.
- We propose a knowledge and geometric filter to discard semantically or spatially improbable relational pairs, which speeds up inference time and makes the framework scalable for large datasets.
- We mitigate the long-tail distribution and lack of label diversity issues by leveraging the captioning capabilities of VLMs and extensive information of LLMs, which allows our framework to control the granularity of the generated scene graph.
- Experiments on downstream tasks, and user evaluations show that our framework can provide semantically meaningful labels, which directly improve SGG training and downstream task performance.

2. Related Work

Fully Supervised SGG: Scene graph generation aims to transform visual data into graph structures, where detected objects serve as nodes and their pairwise relationships define edges. Existing SGG methods often rely on supervised learning from large-scale datasets, such as Visual Genome [21], which can suffer from noisy annotations [25] and long-tailed predicate distributions [37]. To address these limitations, class-aware rebalancing strategies [27] have been proposed to sample training data more evenly across categories, while reweighting techniques [19, 50] incorporate commonsense knowledge to adjust loss weights for different predicates, enhancing model focus on under-represented classes. Despite these advances, fully supervised SGG models remain hindered by noisy and inconsis-

tent annotations, which can degrade the quality of learned representations and limit relational diversity.

Weakly Supervised and Zero-Shot SGG. Weakly supervised SGG aims to develop models capable of generating scene graphs without the requirement of fully annotated datasets. This is often achieved by leveraging image captions to identify and localize triplets of objects and their relationships [17, 56] within images. Despite advances, such approaches typically rely on external datasets for training, and thus inherit their human annotation bias. Besides directly using image-caption pairs for training, prompt tuning [51] can be applied to facilitate SGG and boost fine-grained predicates. Meanwhile, zero-shot SGG has attracted attention. Utilizing models such as CLIP [34] can help to verify the accuracy of relationship predictions and allows for the prediction of relationships even without direct examples in the training data due to the shared embedding space for image and text. This process can be further leveraged with detailed descriptions of visual cues for closed-set relationship detection [26]. Zhao and Xu [57] incorporate commonsense knowledge from foundation models and ConceptGraphs [12] propose a 3D zero-shot SGG by integrating geometric cues and semantic cues from LVLM and LLM respectively. However, limitations remain, such as the focus on spatial predicates only and a dependency on object overlap.

Large Vision and Language Models. VLMs use contrastive learning [16] to align the embedding of vision and language inputs into a single common embedding space which provides remarkable zero-shot performance [45]. Language modeling has recently witnessed significant advances leading to the development of very popular LLMs. As a result of their large-scale training, LLMs have demonstrated impressive zero-shot transferability to downstream tasks such as commonsense reasoning [20, 38, 55]. The development of GPT-3 [6] marked the start of the race towards developing and finetuning LLMs for different language tasks. Most recently, a family of llama 3.2 [38] has been released showing strong performance on different reasoning tasks. We leverage this development and adopt llama 3.2 for the task of caption paraphrasing and triplet extraction due to its remarkable generalization capabilities.

3. Methodology

3.1. Problem Formulation

Scene graph generation (SGG) is a pivotal task in computer vision to construct a structured, graph-based representation of an image's visual content. Formally, a scene graph $G = (V, E)$ consists of a set of nodes $V = \{v_i\}_{i=1}^N$ and directed edges $E = \{e_{ij}\} \subseteq V \times V$. Each node v_i represents an object within the scene, characterized by a label $o_i \in \mathcal{O}$ from a set of object classes \mathcal{O} . Each object v_i



Figure 3. **Qualitative Examples of Scene Graphs:** Input image (middle), Visual Genome’s GT SG (left), and our predicted graph (right). For more examples, please see supplementary material.

is associated with a bounding box $b_i \in \mathbb{R}^4$, which defines its spatial location and extent within the image. The edges $\bar{e}_{ij} = (v_i, v_j, r_{ij})$ encode the relationships between pairs of objects, where $r_{ij} \in \mathcal{R}$ denotes the spatial or semantic relationship from object v_i to object v_j within a set of relation classes \mathcal{R} .

The goal of scene graph generation is, therefore, to predict both the object labels o_i for each node v_i and the relationships r_{ij} for each directed edge e_{ij} , thereby capturing the complex interactions and spatial configurations among objects in a given image I . Given an image $I \in \mathbb{R}^{H \times W}$ with height H , width W , the standard SGG process begins by detecting a set of objects, each associated with a bounding box b_i , and label o_i , which localizes an object within the image, followed by relational inference to establish the relationship r_{ij} between detected object pairs (v_i, v_j) . Given the detected objects and pairwise relations, a set of triplets $T = \{t_i\}_{i=1}^k$ is constructed and the final scene graph G is generated.

3.2. Method Overview

Our proposed scene graph generation (SGG) framework, illustrated in Fig. 2, employs a bottom-up approach for constructing scene graphs (SGs), which allows us to directly convert an input image I to a SG G without relying on extra groundtruth information such as captions. The framework consists of three primary modules: a node prediction module, a caption generation module, and a triplet extraction module. Additionally, it incorporates two auxiliary modules: a geometry filter (\mathcal{GF}), and a relation validation module.

The process begins by analyzing a given input image I , where a set of object nodes v_i is predicted along with their associated bounding boxes b_i and corresponding object labels O_i . Next, a captioning module \mathcal{C} processes pairwise image crops, denoted as I_{ij} , alongside a language prompt p_i , to produce a set of captions c_i that describe relationships between detected objects. These captions are subsequently parsed by a large language model (LLM) to extract a set of possible relational triplets t_i .

To reduce the computational load on the captioning module \mathcal{C} by minimizing the number of object pairs it must analyze, we deploy a geometry filter \mathcal{GF} . The geometry filter (\mathcal{GF}) leverages 2D bounding box information in conjunction with estimated median object depth, derived from a depth estimation module, to infer the 3D center of each bounding box. This 3D center is used to calculate the approximate relative distances between objects in the scene. Object pairs that exceed a defined spatial threshold are deemed irrelevant and are removed from further processing.

Finally, a validation module is incorporated at the end of the pipeline to confirm that the generated set of triplets $T = \{t_i\}$ accurately reflects both spatial and semantic coherence in relation to the input image I .

3.3. Node Prediction Module

The node prediction module is a foundational component of our scene graph generation (SGG) framework, responsible for detecting objects within an input image I and providing precise spatial and categorical information for each identified object. This module outputs a set of object nodes $V = \{v_i\}_{i=1}^N$ with a corresponding set of bboxes $b_i \in \mathbb{R}^4$ and object labels $o_i \in \mathcal{O}$. By accurately locating and labeling each detected object, the node prediction module ensures that subsequent modules, such as caption generation and relation extraction, operate on well-defined, spatially coherent entities.

In cases where the node prediction module fails to detect objects, such as in close-up shots where context may be insufficient, the image I will be discarded, as insufficient object information prevents meaningful processing by subsequent modules.

3.4. Depth Estimation and Geometry Filter

A common approach to scene graph generation (SGG) involves using overlapping bounding boxes to identify pairs of objects that may interact within a scene. However, this method often neglects critical object interactions, potentially omitting key triplets that convey the primary relational context of the scene. For example, in an image depicting two individuals conversing, as illustrated in Fig. 2, a purely overlap-based method would likely miss the principal triplet, *Man, talking to, Man*, due to the non-overlapping nature of their bounding boxes.

While enumerating all possible object pairs could address this issue, it becomes computationally prohibitive in complex scenes with a large number of objects, particularly in our framework, which integrates multiple foundational models. To solve this issue while preserving relational accuracy, we incorporate a depth estimation module and a geometry filter to estimate spatial proximity in a 3D space from a 2D input image I .

The geometry filter estimates the 3D center of each object’s bbox based on spatial and depth information from the input image I and a corresponding depth map D . For each object pair (o_i, o_j) , the 3D bounding box centers are computed, and the pair is retained only if the relative distance between them meets a predefined threshold. The filtering criterion, given by Equation 1, is defined through

$$\lambda_1 \underbrace{(x/y)}_{\text{2D component}} + \lambda_2 \underbrace{\|d_i - d_j\|_2}_{\text{3D component}} < \tau, \quad (1)$$

where x represents the distance between the 2D bounding box centers of objects o_i and o_j , y is the diagonal length of the image, and d_i, d_j denote the normalized median depths for o_i and o_j , respectively. The hyperparameters λ_1 and λ_2 control the relative contributions of the 2D and 3D components, while $\tau > 0$ represents the threshold for retaining pairs.

By filtering object pairs based on 2D spatial proximity and relative depth in 3D space, these combined modules reduce the number of object pairs that must be processed by the captioning module \mathcal{C} , focusing on spatially coherent, contextually relevant pairs. This approach significantly enhances the computational efficiency of our framework while ensuring that only meaningful relational information is retained.

3.5. Caption Generation Module

At the core of our proposed framework lies the Caption Generation Module \mathcal{C} . Given m detected object nodes $V = \{v_1, v_2, \dots, v_m\}$ within an input image, our caption generation module systematically formulates object pairing proposals by iterating over all unique object combinations. Given the typical training of vision-language models, such

as Up-Down [3] and BLIP [24], the models primarily produce captions interpreting the overall context of a given image, not focusing exclusively on the finer details pertaining to object-object interactions, which are vital for SGG.

To adequately direct the model’s attention to the object pair in question, we create a focused image crop containing the object pair to capture their specific interaction within a localized context. Inspired by [36], we highlight both objects using distinct visual cues (red and yellow bboxes) to shift the model’s attention to the relevant objects and their interaction. To further improve the clarity and contextual focus of the generated captions, we employ a structured language prompt provided to the VLM, following inspiration from different prompting technique [31, 32, 42]:

“What is the relationship between the {obj1} in the red rectangle and the {obj2} in the yellow rectangle? Use the red and yellow rectangle to locate the objects, and then focus primarily on understanding the pairwise relation between the {obj1} in the red rectangle and the {obj2} in the yellow rectangle, in a way that reflects their interaction or relative location.”

where {obj1} and {obj2} are dynamically replaced with the names of the detected objects (e.g., *person, dog*), reinforcing the prompt’s emphasis on the specific interaction between the highlighted objects.

The VLM processes each annotated image crop, generating a set of descriptive captions conveying detailed relational context for each object pair. The pairwise-captions provide rich semantics and carry potential relation information which are then extracted with the help of the Triplet Extraction Module. This module facilitates the extraction of fine-grained relational information by guiding the VLM to focus on specific pairwise interactions, enabling a detailed and contextually coherent representation of relationships within the scene.

3.6. Triplet Extraction Module

Our proposed framework follows a bottom-up paradigm, facilitating the efficient extraction of relational triplets once object categories are set earlier in the pipeline. To harness the extensive linguistic and contextual understanding embedded in LLMs, we employ a two-step prompting strategy. In this approach, the LLM is first prompted to paraphrase pairwise captions, after which the paraphrased output is leveraged to support precise triplet extraction.

For instance, consider a sample caption such as *“two men engaged in a conversation”*, as shown in Fig. 2. Prompting the LLM to extract a triplet directly from this caption may yield ambiguous results, such as *“[two men, talking, each other]”*, which lacks sufficient clarity to be accurately mapped to the input image I . By applying the two-step prompting process in a Chain of Thought (CoT) [42]

approach, the LLM reformulates the caption into a more explicit form, such as "a man is talking to a man", enabling the straightforward extraction of the triplet "[man, talking to, man]". This two-step approach, therefore, enhances the extraction process, yielding relational triplets that more precisely capture the core visual interactions. For further details on the prompts, please refer to the supplementary material.

3.7. Relation Validation Module

To ensure that the extracted triplets are both semantically and spatially relevant to the input image I , our framework integrates a relation validation module employing a Visual Question Answering (VQA) [4] model for targeted validation. While using the CLIPScore metric [13] offers a means to check alignment between image content and text by evaluating caption relevance, CLIP [34] has been shown to have limitations in understanding nuanced semantics within images [54]. Consequently, using CLIPScore for triplet validation often yields inconsistent results.

Given these challenges, our approach opts for a more direct validation technique. For each extracted triplet $\bar{e}_{ij} = (v_i, v_j, r_{ij})$ - where v_i and v_j represent detected object nodes and r_{ij} the proposed relation - our VQA model is prompted with a binary question specific to the triplet in the form of "Is the subject relationship the object?", querying whether the relation r_{ij} between v_i and v_j accurately describes their interaction or spatial arrangement in I . The triplet is retained or discarded based on the binary answer of the VQA model.

The resulting set of validated triplets contains only relations confirmed as semantically and spatially coherent within the context of the input image, enabling downstream processes to leverage a reliable set of object interactions.

4. Experiments

Datasets. For Scene Graph Generation (SGG), we use the original test split from the Visual Genome dataset [21] and conduct an extensive user study to assess qualitative aspects. For Sentence-to-Graph Retrieval, we adopt the setup outlined in [37], which leverages a dataset of 51k overlapping images between Visual Genome and MS-COCO Caption [30]. This combined dataset is split into 35k images for training, 1k images for validation, and 5k images for testing. We evaluate on a gallery size of 1k and 5k respectively as the original setup [37]. For Image Captioning, we use the MS-COCO dataset [30], which contains over 330k images, each annotated with five captions. We specifically evaluate on the 5,000-image test set provided in the Karpathy split [15].

Implementation Details and Foundation Models.

Node Prediction Module. We adopted Florence-2 [43], a lightweight model that is trained with a unified represen-

tation. We run the object detection task using the large-ft version of the model with sdpa [39] attention with no post-processing.

Depth Estimation Module. We deployed the base version of Depth-Anything-V2 [46] as it features fast inference speed at high depth accuracy.

Geometry Filter. Parameters are set to $\lambda_1 = 0.5$; $\lambda_2 = 1$; $\tau = 0.45$.

Caption Generation Module. We use LLaVA-OneVision[23] with a batch size of 15, maximum output token of 50, and number of beams equal to 1.

Triplet Extraction Module. We exploit the strong reasoning capabilities of the llama 3.2 model family [1]. We deploy the 3B version of the model with a batch size of 16, maximum output tokens of 256 to allow processing a large subset of captions at once.

Relation Validation Module. We deploy LLaVA-OneVision[23] as a VQA model to benefit from its improved reasoning capabilities in filtering out semantically meaningless relations. Fig. 3 shows visual comparison between SGs generated by PRISM-0 and their VG counterparts. By visual inspection, we can notice that SGs generated by PRISM-0 focus on the semantics of the scene while also providing fine-grained details. For more visualizations, please refer to the supplementary material.

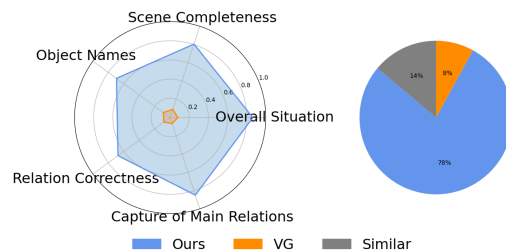


Figure 4. **Subjective Quality of Generated Scene Graph.** The radar plot (left) illustrates the average normalized scores from human evaluation across five evaluation aspects. The pie chart (right) represents the overall preference distribution, each color indicates the percentage of users who consider the corresponding methods more descriptive in the pre-defined aspects. Preference for PRISM-0 is blue while VG is indicated orange. The gray segment represents the percentage of users who found both methods equally descriptive.

4.1. Qualitative Evaluation

In this section, we conduct a thorough qualitative evaluation of a subset of the scene graphs generated by PRISM-0 and compare against GT annotations. We conducted a user study involving 75 participants from diverse backgrounds. Each participant evaluated 40 randomly selected images along with their corresponding SGs. They rated the graphs based on five criteria: overall perception of the graph (Over-

all Situation), node accuracy (Object Names), Scene Completeness, perceptual precision (Relation Correctness), and perceptual recall (Capture of Main Relation).

The survey result is summarized in Fig. 4, illustrating that our approach significantly outperforms VG annotations under subjective assessment across all five metrics. Specifically, the semantic scene relations (completeness, situation, main relations) stand out. Fig. 3 depicts

Statistical Analysis. We applied a paired sample t-test to the survey scores to confirm our statistical improvement. The test results showed significant enhancements in all five categories ($p < 0.05$), reinforcing the qualitative feedback from the user study.

4.2. Quantitative Evaluation on Downstream Tasks

We validate the effectiveness of PRISM-0 by demonstrating its application on two vision-language downstream tasks: Image Captioning, and Sentence-to-Graph Retrieval (S2GR). Traditional SGG evaluation benchmarks such as predicate classification, SG detection, and SG classification, are unsuitable for our zero-shot framework, which explicitly avoids dependence on the existing VG annotation to overcome the inherent bias and the lack of diversity in predicate categories. Instead, we focus on downstream applications that use SGs to enrich task-specific outputs, with S2GR and image captioning as our primary tasks.

Sentence to Graph Retrieval (S2GR). S2GR was initially proposed by [37] to evaluate graph-level coherence. It parses the human-provided caption into a text graph, which is then used as a query to retrieve scene graphs (SGs) that represent images with similar visual concepts. In S2GR, the concept of image visual features is disregarded, and only SGs are considered a valid representation of an image. The text-SGs used as retrieval queries are created by parsing GT captions from the MS-COCO dataset [30].

We adopt the implementation from [37] and report two key evaluation metrics: meanRecall@20/100 (R@20/100) and the median ranking index (Med) on a gallery size of 1,000 and 5,000. We compare our model with the top-performing Motif-based TDE (MTDE) model from [37]. Additionally, we also compare against state-of-the-art supervised SGG models, including CaCao [51], which fine-tunes a visually-prompted language model; LLM4SGG [18], which leverages VLMs to generate weak labels for training a supervised SGG model; and PGSG [28], which trains a VLM to generate SGs directly from input images and GT captions.

As shown in Table 1, our model significantly outperforms the best-performing TDE model, which struggles with predicate diversity. We also outperform PGSG and CaCao, even though these models are trained on MS-COCO [30] captions. However, we rank second to LLM4SGG. We believe this is due to the fact that they utilize MS-COCO

GT captions to generate weak labels by parsing captions into triplets, which are then used to train a fully supervised SGG model. This process results in their output being more closely aligned with queries originally parsed from captions in the same dataset, yielding a higher retrieval accuracy.

Table 1. Performance comparison of Sentence-to-Graph Retrieval. ZS refers to the approach being fully zero-shot.

Model	Size	1000			5000		
	ZS	R@20	R@100	Med	R@20	R@100	Med
MTDE	✗	17.0	53.6	91	5.2	18.9	425
PGSG	✗	48.4	75.3	97	27.1	54.3	313
CaCao	✗	52.0	77.3	85	33.4	60.9	322
LLM4SGG	✗	56.9	82.9	64	34.0	64.8	211
Ours	✓	56.9	80.2	71	32.6	64.0	223

Image Captioning. To assess the effectiveness of PRISM-0 as a holistic graph representation for the image, we conduct an image captioning experiment where the generated scene graphs serve as auxiliary information alongside visual features to generate captions. Scene graph-based image captioning models normally starts with scene graph generation, where object and pairwise relations are predicted. The resulting scene graph is then used to guide the generation of captioning as an explicit relationship representation of the image. Traditional methods typically rely on standard supervised methods to obtain the intermediate scene graph, pre-trained on VG labels. Our implementation is based on the code base [58]. The relation prediction is combined with the visual features derived by [3] to provide node and edge features. We transform relation predictions into close-set predicates. For evaluation, we adhere to standard protocols employing the following metrics: BLEU [33], METEOR [5], CIDER [40], ROUGE [29] and SPICE [2] as metrics to evaluate the quality of image captioning. As shown in Table 2, we outperform the baseline of Full-GC on all 6 metrics by introducing external relation prediction on all pairwise predictions. However, while we observe gains over the baseline by leveraging our enhanced scene graph representations, our results are still not comparable with state-of-the-art methods such as TSG [48], which achieve significantly higher performance in CIDER and SPICE metrics.

4.3. Ablation Study

We perform an ablation study to evaluate the impact of different framework modules on the generated scene graphs. We evaluate the predicted scene graphs for the downstream task of S2GR and report the results in Table 3.

Geometric filter. Fig. 5 illustrates the effectiveness of the geometric filter in pruning irrelevant connections from the output scene graph, preserving only edges that represent meaningful relationships. This refinement improves perfor-

Table 2. Performance comparison of Image Captioning.

Method	B1	B4	C	R	M	S
Up-Down[3]	77.2	36.2	113.5	56.4	27.0	20.3
GCN-LSTM[49]	77.3	36.8	116.3	57.0	27.9	20.9
SGAE[47]	77.6	36.9	116.7	57.2	27.7	20.9
TSG	-	38.1	120.2	57.7	28.6	21.9
MFN-SGC	76.8	36.2	115.3	56.6	27.7	20.7
MFN-FGC	76.7	36.9	114.8	56.8	27.9	20.8
Ours-FGC	76.8	37.1	115.3	56.9	28.0	20.8

Table 3. Ablation study for framework components. Evaluated on downstream task S2GR with a gallery size of 1000 images.

Model Change	R@20	R@100	Med
w/o Geometric Filter	29.8	61.1	239
LLM (3B \rightarrow 1B)	50.8	72.4	126
w/ VG GT Objects	59.3	81.4	70
Ours (Full Pipeline)	59.3	81.4	70

mance in downstream tasks such as S2GR. As shown in Table 3. Removing the geometric filter results in a significant decline in retrieval performance, due to cluttered scene graphs with inaccurate relations. Furthermore, the geometric filter plays a critical role in reducing the computational overhead for both the VLM and LLM, thereby accelerating the inference process, as shown in Table 4.

Table 4. Average inference time per image with and without the Geometric filter.

Model	Avg. time (sec)
w/o Geometric Filter	90.0
w/ Geometric Filter	67.5

Large Language Model. We replace the llama 3.2 3B model with a smaller 1B version to test the significance of LLM size on the final generated graphs. As Table 3 shows, switching to a smaller model leads to a performance drop in the retrieval task, which is due to the model’s inability to correctly extract the relations from the provided captions and limited paraphrasing capabilities.

VG Groundtruth Bounding Boxes. In this experiment we drop our node prediction module and use the ground truth bounding boxes from VG. The consistent performance of our pipeline suggests that our node detection model is performing on par with the ground truth annotations.

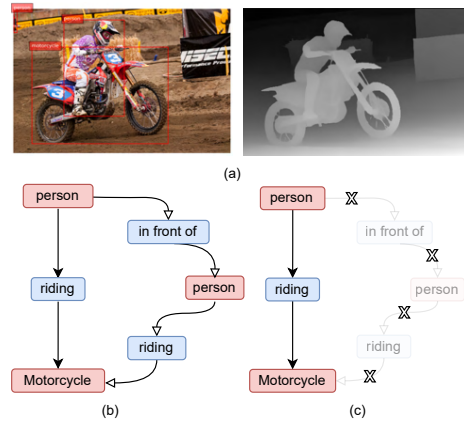


Figure 5. **Applying Geometric Filter for Scene Graph Generation.** (a) shows RGB image (left) with detected objects including one person in the background in the top left corner and the corresponding depth map (right). (b) illustrates the initial scene graph, including unreasonable relations like "person in front of person" and "person riding motorcycle" due to distant spatial positioning. (c) shows the refined graph after filtering out implausible relations based on geometry, resulting in a more accurate representation.

5. Limitations & Conclusion

Limitation. While our proposed framework demonstrates promising results, several limitations should be acknowledged. First, the performance of the system relies on the quality and accuracy of the node prediction module. In scenarios where object detection fails, the system’s ability to generate meaningful scene graphs is significantly impeded. Second, despite the application of filters like the *Geometric Filter* and *Validation Module*, the model can struggle with handling complex relational dynamics between distant or visually ambiguous objects. Third, the reliance on large-scale pre-trained models introduces computational overhead and complexity, which limit real-time performance or applications in resource-constrained environments.

Conclusion. In this work, we introduce PRISM-0, a zero-shot framework for Scene Graph Generation (SGG) that utilizes a bottom-up approach to produce richer, more comprehensive scene graphs. Our method addresses the limitations of existing SGG datasets, which often suffer from sparse annotations and noisy labels, by enhancing the graph’s quality. PRISM-0 is modular and leverages state-of-the-art Vision-Language Models (VLMs) and Large Language Models (LLMs), ensuring that the framework benefits from advancements in vision-language pre-training. We demonstrate that, despite being fully zero-shot, PRISM-0 outperforms existing methods in downstream tasks that require high relational diversity.

PRISM-0: A Predicate-Rich Scene Graph Generation Framework for Zero-Shot Open-Vocabulary Tasks

Supplementary Material

6. Ablation Studies: Framework Modules

In this section, we extend our ablation study to assess the impact of additional modules in the framework on the overall performance of the pipeline. Table 5 builds upon Table 3, demonstrating the effects of ablations on the downstream task of Scene-to-Graph Retrieval (S2GR) with a gallery size of 1000 images.

Depth Estimation As shown in the table, replacing Depth-Anything-V2 [46] with the less-performing Monodepth2 [10] model results in a performance drop. This can be attributed to the generation of incorrect graph edges, as shown in Fig. 5, or the creation of overly cluttered scene graphs containing irrelevant information, which adversely affects retrieval rates.

Node Prediction Replacing the Florence-2 [43] detection model with a weaker model, such as YOLOv3 [35], decreases S2GR performance. This decline may be attributed to the limited object categories these models were trained on, lower detection accuracy, or both.

Captioning Model. Replacing Llava-Onevision [23] with Blip3 [44] as the captioning model results in decreased performance. Upon examining the quality of the generated captions, we observed that Blip3 produces less diverse outputs compared to Llava-Onevision, often generating highly similar captions for different crops of the same image, regardless of the highlighted objects. This lack of diversity may explain the observed performance drop.

Captioning Approach The results also indicate that changing the captioning approach from cropped images with highlighted objects to entirely masking the rest of the image, while retaining only the objects of interest, negatively impacts the performance. Masking removes additional scene context, which can enhance performance when the context is irrelevant. However, eliminating all contextual information between objects may discard critical relational cues, potentially explaining the observed drop in retrieval rates.

Similarly, employing Chain-of-Thought (CoT) prompting for VLMs may introduce extra contextual information, which could mislead the model during caption generation. The specific prompt used for CoT-based captioning is as follows:

The text in backticks represents the caption that you provided for this image. In light of that caption, Please describe the relation between the

{obj1} in the red box and the {obj2} in the yellow rectangle. The text: "full-caption"

Validation Module Lastly, removing the validation module negatively impacts the outcome, highlighting its crucial role in pruning generated scene graphs.

Table 5. More Ablations of different framework modules. Evaluated on downstream task S2GR with a gallery size of 1000 images.

Model Change	R@20	R@100	Med
w/o Geometric Filter	29.8	61.1	239
w/o Validation module	50.1	69.4	140
LLM (3B \rightarrow 1B)	50.8	72.4	126
Depth Estimator	52.9	73.4	121
Captioning Model	53.2	77.2	104
Captioning w/ masks	53.7	79.4	74
Captioning w/ CoT	54.5	77.6	100
Detection Model	59.3	78.7	100
w/ VG GT Objects	59.3	81.4	70
Ours (Full Pipeline)	59.3	81.4	70

7. LLM Prompts for Triplet Extraction

We utilized prompts designed for LLMs to derive meaningful triplets that describe relationships between objects in an image. The process involves a combination of paraphrasing and extraction steps, supported by Chain-of-Thought [42] and in-context learning [6] techniques. The following task description outlines this approach in detail:

"The goal is to identify and extract structured triplets in the format (subject, predicate, object) from the provided sentence. The subject and object must correspond to specific object class names explicitly mentioned at the end of the query. To achieve this, follow a two-step approach: Rephrase the sentence: Simplify the sentence to focus on the key interaction or relationship between the subject and the object. Extract the triplet: Based on the rephrased sentence, identify and output the triplet in the specified format. The subject refers to the entity initiating an action or being described, while the object refers to the entity affected by or connected to the action. The predicate represents the action or relationship connecting the subject and object. En-

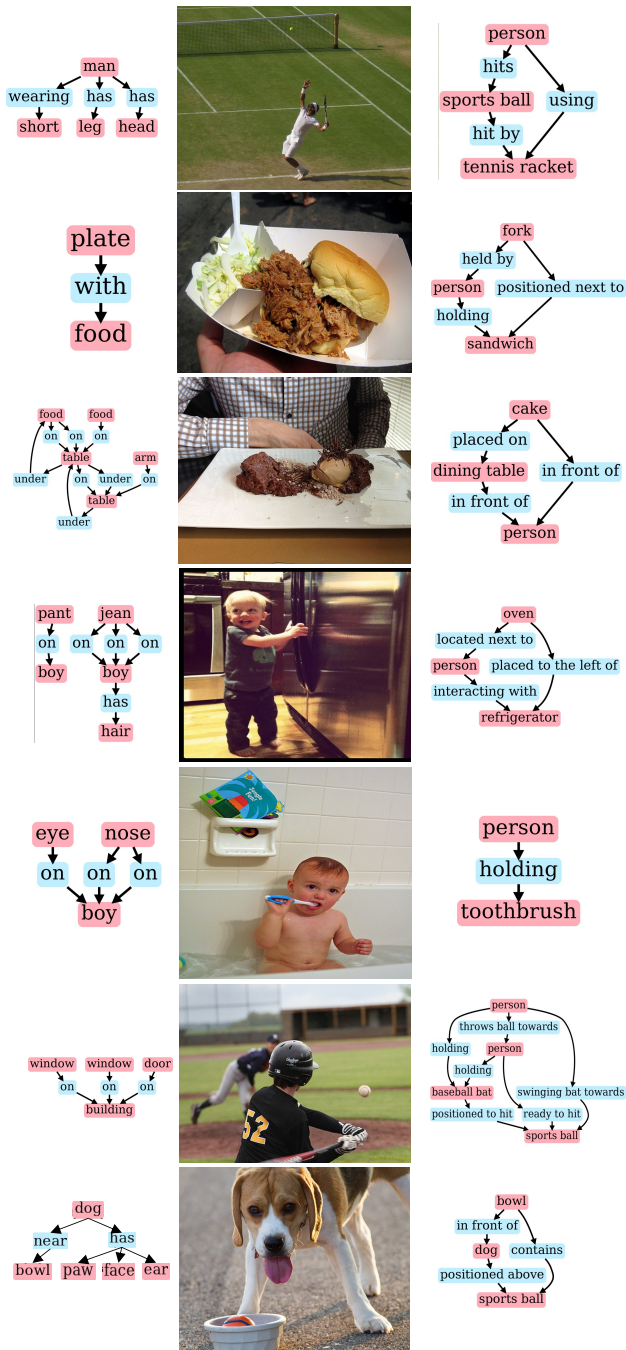


Figure 6. **More qualitative Examples of Scene Graphs:** Input image (middle), Visual Genome’s GT SG (left), and our predicted graph (right). For more examples.

sure that the subject and object match the exact class names mentioned in the question.”

In-Context Examples for Guiding LLM Behavior To enhance the accuracy of triplet extraction, we provided sev-

eral in-context examples that illustrate both the paraphrasing and extraction steps. These examples help the LLM understand the expected output format and the logical flow of reasoning required for accurate triplet identification. The following is the in-context examples we provided to the LLM:

Question 1: Given the sentence "Two men sit on a bench near the sidewalk and one of them talks on a cell phone.", extract meaningful triplets describing the relationship between person and person.

Answer 1: Step 1: The sentence can be paraphrased as: One person is sitting on a bench. The other person is also seated on the bench near the road. One person is talking on a mobile phone. Step 2: Meaningful triplets, where the subject and object are the simple noun, extracted from the paraphrased sentence are: <person, next to, person>.

Question 2: Given the sentence "The banana is not directly related to the car. This arrangement creates a visually interesting contrast between the two objects, as the banana is a fruit and the car is in the same image.", extract meaningful triplets describing the relationship between Banana and car.

Answer 2: Step 1: The sentence can be paraphrased as: The Banana is not directly related to car. Step 2: It is not possible to extract triplets for the given pair because there is no meaningful triplet for the given two objects.

User: Predicates such as 'not directly related to', 'in the same environment as', 'part of the same team as', 'in the same group as', 'in the same team as', 'not related to' do not have a semantic or geometric meaning.

Question 3: Given the sentence "The woman in the red rectangle is a photographer on the right, who is holding a camera and taking pictures. The backpack in the yellow rectangle is placed on the

ground near another photographer on the left. Both photographers are part of the same event and are taking photos in a similar area.", extract meaningful triplets describing the relationship between the woman in the red rectangle and the backpack in the yellow rectangle."

Answer 3: Step 1: The sentence can be paraphrased as: The woman in the red rectangle is positioned on the right side, taking photos, while the backpack in the yellow rectangle is on the ground near the photographer on the left. The woman in the red rectangle is positioned to the right of the backpack in the yellow rectangle. Step 2: Meaningful triplets, where the subject and object are the simple noun, extracted from the paraphrased sentence are: <woman in the red rectangle, stands on the right of, backpack in the yellow rectangle>.

The in-context examples were designed to guide the LLMs in handling various scenarios during triplet extraction. The first example demonstrates how to process sentences that lack an explicit predicate, such as a verb or adjective, describing the relationship between the objects of interest. In such cases, the LLM is instructed to reason and paraphrase the sentence into a more structured and extractable format.

The second example instructs the LLM to discard sentences containing vague or semantically meaningless relations, such as "not directly related to" or "in the same group as," ensuring only meaningful relationships are retained.

The third example addresses scenarios where the relationship between two objects can be inferred through their connection to a common object in the scene. For example, in the third example, the LLM analyzes the spatial and contextual relationships by identifying their individual connections to the other photographer (a common object), the LLM infers the spatial relationship between the woman and the backpack. This reasoning leads to the triplet {woman in the red rectangle, stands on the right of, backpack in the yellow rectangle}. Furthermore, the use of descriptive references like "in the red rectangle" or "in the yellow rectangle" mirrors the actual captions processed by the LLM, as these captions often include bounding box annotations (e.g., red and yellow rectangles) around the objects of interest. This alignment ensures the training examples reflect real-world usage, enhancing the LLM's ability to extract accurate and

meaningful triplets.

The combination of CoT prompting and in-context examples can significantly improve the LLM's ability to extract accurate and semantically meaningful triplets, making it a valuable component of the PRISM-0 framework for zero-shot open-vocabulary scene graph generation.

8. User Study Details

This section provides detailed insights into the study presented in 4.1 in terms of the setup, the concepts, and the participants' demographics.

Figure 7 serves as the foundational introduction for participants, explaining key concepts required for the evaluation. It clarifies the distinctions between factual relations, main relations, minor relations, and non-factual relations, using illustrative examples. These explanations ensure participants have a consistent understanding of the relational criteria used to evaluate scene graphs, enabling meaningful comparisons between PRISM-0 results and VG ground truth.

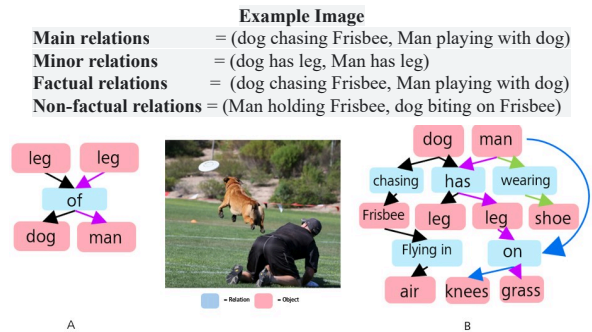


Figure 7. **Illustration of user study concepts:** This figure explains foundational concepts such as factual relations vs non-factual relations, main vs minor relations.

The core evaluation task is depicted in Figure 8. Participants were shown a reference image accompanied by two scene graphs, labeled A and B. One graph represents PRISM-0's predictions, while the other shows the Visual Genome ground truth. To minimize positional bias, the order of the graphs (A or B) was randomized across different questions. Participants assessed these graphs based on predefined aspects of scene understanding, such as scene completeness, relational accuracy, capture of main relations, and object names.

Figures 9 and 10 provide demographic information about the participants in the study. Figure 9 illustrates the age distribution of the participants, ensuring a diverse age range. Figure 10 shows the highest degree achieved by the participants, highlighting their qualifications.

Please choose which graph is **better** in the following 5 aspects. *

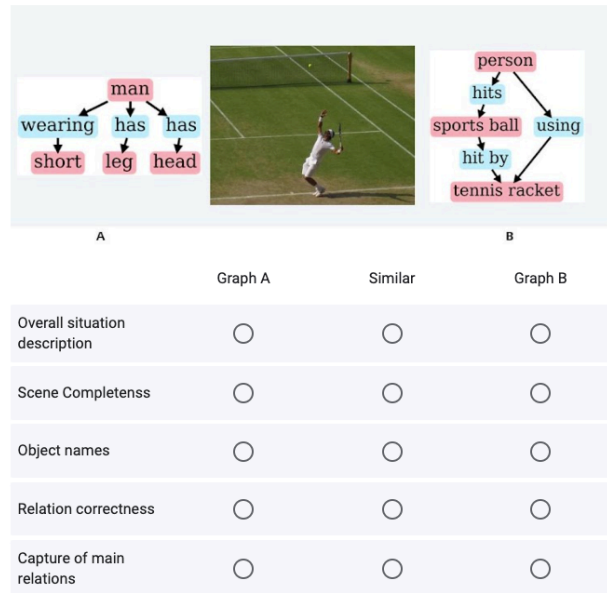


Figure 8. **User study question example:** The middle panel shows the reference image, with scene graph A and scene graph B displayed on either side. One represents our result, while the other is the Visual Genome ground truth. The order of scene graphs is randomized for different questions.

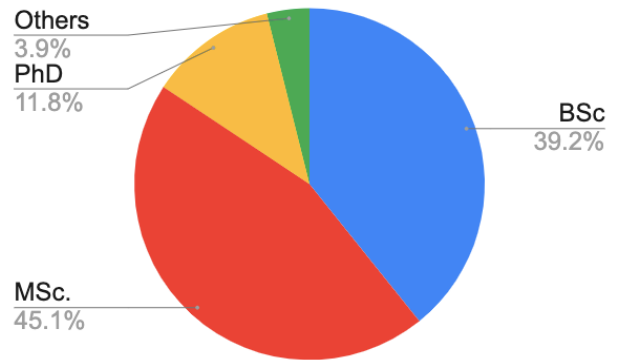


Figure 10. **User Study Highest Degree Distribution**

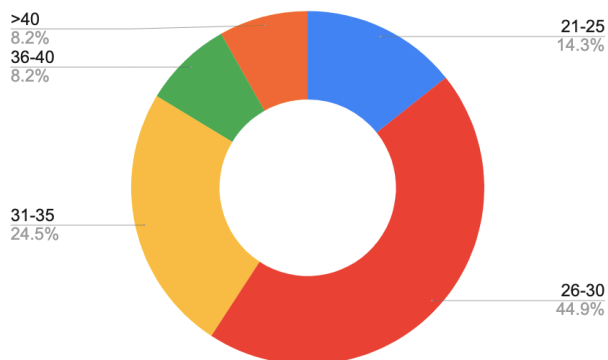


Figure 9. **User Study Age Distribution**

References

- [1] Meta AI. Llama 3.2: Connect 2024 – vision at the edge for mobile devices, 2024. Accessed: 2024-11-14. 6
- [2] Peter Anderson, Basura Fernando, Mark Johnson, and Stephen Gould. Spice: Semantic propositional image caption evaluation. In *Computer Vision–ECCV 2016: 14th European Conference, Amsterdam, The Netherlands, October 11–14, 2016, Proceedings, Part V 14*, pages 382–398. Springer, 2016. 7
- [3] Peter Anderson, Xiaodong He, Chris Buehler, Damien Teney, Mark Johnson, Stephen Gould, and Lei Zhang. Bottom-up and top-down attention for image captioning and visual question answering. In *Proceedings of the IEEE conference on computer vision and pattern recognition*, pages 6077–6086, 2018. 5, 7, 8
- [4] Stanislaw Antol, Aishwarya Agrawal, Jiasen Lu, Margaret Mitchell, Dhruv Batra, C Lawrence Zitnick, and Devi Parikh. Vqa: Visual question answering. In *Proceedings of the IEEE international conference on computer vision*, pages 2425–2433, 2015. 6
- [5] Satanjeev Banerjee and Alon Lavie. Meteor: An automatic metric for mt evaluation with improved correlation with human judgments. In *Proceedings of the acl workshop on intrinsic and extrinsic evaluation measures for machine translation and/or summarization*, pages 65–72, 2005. 7
- [6] Tom Brown, Benjamin Mann, Nick Ryder, Melanie Subbiah, Jared D Kaplan, Prafulla Dhariwal, Arvind Neelakantan, Pranav Shyam, Girish Sastry, Amanda Askell, et al. Language models are few-shot learners. *Advances in neural information processing systems*, 33:1877–1901, 2020. 3, 1
- [7] Xiaojun Chang, Pengzhen Ren, Pengfei Xu, Zhihui Li, Xiaojiang Chen, and Alex Hauptmann. A comprehensive survey of scene graphs: Generation and application. *IEEE Transactions on Pattern Analysis and Machine Intelligence*, 45(1): 1–26, 2021. 1
- [8] Helisa Dhama, Azade Farshad, Iro Laina, Nassir Navab, Gregory D Hager, Federico Tombari, and Christian Rupprecht. Semantic image manipulation using scene graphs. In *Proceedings of the IEEE/CVF conference on computer vision and pattern recognition*, pages 5213–5222, 2020. 1
- [9] Helisa Dhama, Fabian Manhardt, Nassir Navab, and Federico Tombari. Graph-to-3d: End-to-end generation and manipulation of 3d scenes using scene graphs. In *Proceedings of the IEEE/CVF International Conference on Computer Vision*, pages 16352–16361, 2021. 1
- [10] Clément Godard, Oisín Mac Aodha, Michael Firman, and Gabriel J Brostow. Digging into self-supervised monocular depth estimation. In *Proceedings of the IEEE/CVF international conference on computer vision*, pages 3828–3838, 2019. 1
- [11] Nishad Gothoskar, Marco Cusumano-Towner, Ben Zinberg, Matin Ghavamizadeh, Falk Pollok, Austin Garrett, Josh Tenenbaum, Dan Gutfreund, and Vikash Mansinghka. 3dp3: 3d scene perception via probabilistic programming. *Advances in Neural Information Processing Systems*, 34:9600–9612, 2021. 1
- [12] Qiao Gu, Alihusein Kuwajerwala, Sacha Morin, Krishna Murthy Jatavallabhula, Bipasha Sen, Aditya Agarwal, Corban Rivera, William Paul, Kirsty Ellis, Rama Chellappa, et al. Conceptgraphs: Open-vocabulary 3d scene graphs for perception and planning. *arXiv preprint arXiv:2309.16650*, 2023. 3
- [13] Jack Hessel, Ari Holtzman, Maxwell Forbes, Ronan Le Bras, and Yejin Choi. Clipscore: A reference-free evaluation metric for image captioning. *arXiv preprint arXiv:2104.08718*, 2021. 6
- [14] Justin Johnson, Agrim Gupta, and Li Fei-Fei. Image generation from scene graphs. In *Proceedings of the IEEE conference on computer vision and pattern recognition*, pages 1219–1228, 2018. 1
- [15] Andrej Karpathy and Li Fei-Fei. Deep visual-semantic alignments for generating image descriptions. In *Proceedings of the IEEE conference on computer vision and pattern recognition*, pages 3128–3137, 2015. 6
- [16] Prannay Khosla, Piotr Teterwak, Chen Wang, Aaron Sarna, Yonglong Tian, Phillip Isola, Aaron Maschiot, Ce Liu, and Dilip Krishnan. Supervised contrastive learning. *Advances in neural information processing systems*, 33:18661–18673, 2020. 3
- [17] Kibum Kim, Kanghoon Yoon, Jaehyeong Jeon, Yeonjun In, Jinyoung Moon, Donghyun Kim, and Chanyoung Park. Llm4sgg: Large language model for weakly supervised scene graph generation. *arXiv e-prints*, pages arXiv–2310, 2023. 2, 3
- [18] Kibum Kim, Kanghoon Yoon, Jaehyeong Jeon, Yeonjun In, Jinyoung Moon, Donghyun Kim, and Chanyoung Park. Llm4sgg: Large language models for weakly supervised scene graph generation. In *Proceedings of the IEEE/CVF Conference on Computer Vision and Pattern Recognition*, pages 28306–28316, 2024. 7
- [19] Boris Knyazev, Harm De Vries, Cătălina Cangea, Graham W Taylor, Aaron Courville, and Eugene Belilovsky. Graph density-aware losses for novel compositions in scene graph generation. *arXiv preprint arXiv:2005.08230*, 2020. 3
- [20] Takeshi Kojima, Shixiang Shane Gu, Machel Reid, Yutaka Matsuo, and Yusuke Iwasawa. Large language models are zero-shot reasoners. *Advances in neural information processing systems*, 35:22199–22213, 2022. 3
- [21] Ranjay Krishna, Yuke Zhu, Oliver Groth, Justin Johnson, Kenji Hata, Joshua Kravitz, Stephanie Chen, Yannis Kalantidis, Li-Jia Li, David A Shamma, et al. Visual genome: Connecting language and vision using crowdsourced dense image annotations. *International journal of computer vision*, 123:32–73, 2017. 1, 2, 3, 6
- [22] Stan Weixian Lei, Difei Gao, Jay Zhangjie Wu, Yuxuan Wang, Wei Liu, Mengmi Zhang, and Mike Zheng Shou. Symbolic replay: Scene graph as prompt for continual learning on vqa task. In *Proceedings of the AAAI Conference on Artificial Intelligence*, pages 1250–1259, 2023. 1
- [23] Bo Li, Yuanhan Zhang, Dong Guo, Renrui Zhang, Feng Li, Hao Zhang, Kaichen Zhang, Yanwei Li, Ziwei Liu, and Chunyuan Li. Llava-onevision: Easy visual task transfer. *arXiv preprint arXiv:2408.03326*, 2024. 6, 1

- [24] Junnan Li, Dongxu Li, Caiming Xiong, and Steven Hoi. Blip: Bootstrapping language-image pre-training for unified vision-language understanding and generation. In *International conference on machine learning*, pages 12888–12900. PMLR, 2022. 5
- [25] Lin Li, Long Chen, Yifeng Huang, Zhimeng Zhang, Songyang Zhang, and Jun Xiao. The devil is in the labels: Noisy label correction for robust scene graph generation. In *Proceedings of the IEEE/CVF Conference on Computer Vision and Pattern Recognition*, pages 18869–18878, 2022. 3
- [26] Lin Li, Jun Xiao, Guikun Chen, Jian Shao, Yueting Zhuang, and Long Chen. Zero-shot visual relation detection via composite visual cues from large language models. *Advances in Neural Information Processing Systems*, 36, 2024. 3
- [27] Rongjie Li, Songyang Zhang, Bo Wan, and Xuming He. Bipartite graph network with adaptive message passing for unbiased scene graph generation. In *Proceedings of the IEEE/CVF Conference on Computer Vision and Pattern Recognition*, pages 11109–11119, 2021. 3
- [28] Rongjie Li, Songyang Zhang, Dahua Lin, Kai Chen, and Xuming He. From pixels to graphs: Open-vocabulary scene graph generation with vision-language models. In *Proceedings of the IEEE/CVF Conference on Computer Vision and Pattern Recognition*, pages 28076–28086, 2024. 2, 7
- [29] Chin-Yew Lin. Rouge: A package for automatic evaluation of summaries. In *Text summarization branches out*, pages 74–81, 2004. 7
- [30] Tsung-Yi Lin, Michael Maire, Serge Belongie, James Hays, Pietro Perona, Deva Ramanan, Piotr Dollár, and C Lawrence Zitnick. Microsoft coco: Common objects in context. In *Computer Vision–ECCV 2014: 13th European Conference, Zurich, Switzerland, September 6–12, 2014, Proceedings, Part V 13*, pages 740–755. Springer, 2014. 6, 7
- [31] Pengfei Liu, Weizhe Yuan, Jinlan Fu, Zhengbao Jiang, Hiroaki Hayashi, and Graham Neubig. Pre-train, prompt, and predict: A systematic survey of prompting methods in natural language processing. *ACM Computing Surveys*, 55(9): 1–35, 2023. 5
- [32] Timothy E Morse and John W Schuster. Simultaneous prompting: A review of the literature. *Education and Training in Developmental Disabilities*, pages 153–168, 2004. 5
- [33] Kishore Papineni, Salim Roukos, Todd Ward, and Wei-Jing Zhu. Bleu: a method for automatic evaluation of machine translation. In *Proceedings of the 40th annual meeting of the Association for Computational Linguistics*, pages 311–318, 2002. 7
- [34] Alec Radford, Jong Wook Kim, Chris Hallacy, Aditya Ramesh, Gabriel Goh, Sandhini Agarwal, Girish Sastry, Amanda Askell, Pamela Mishkin, Jack Clark, et al. Learning transferable visual models from natural language supervision. In *International conference on machine learning*, pages 8748–8763. PMLR, 2021. 3, 6
- [35] Joseph Redmon. Yolov3: An incremental improvement. *arXiv preprint arXiv:1804.02767*, 2018. 1
- [36] Aleksandar Shtedritski, Christian Rupprecht, and Andrea Vedaldi. What does clip know about a red circle? visual prompt engineering for vlms. In *Proceedings of the IEEE/CVF International Conference on Computer Vision*, pages 11987–11997, 2023. 5
- [37] Kaihua Tang, Yulei Niu, Jianqiang Huang, Jiaxin Shi, and Hanwang Zhang. Unbiased scene graph generation from biased training. In *Conference on Computer Vision and Pattern Recognition*, 2020. 3, 6, 7
- [38] Hugo Touvron, Louis Martin, Kevin Stone, Peter Albert, Amjad Almahairi, Yasmine Babaei, Nikolay Bashlykov, Soumya Batra, Prajjwal Bhargava, Shruti Bhosale, et al. Llama 2: Open foundation and fine-tuned chat models. *arXiv preprint arXiv:2307.09288*, 2023. 3
- [39] A Vaswani. Attention is all you need. *Advances in Neural Information Processing Systems*, 2017. 6
- [40] Ramakrishna Vedantam, C Lawrence Zitnick, and Devi Parikh. Cider: Consensus-based image description evaluation. In *Proceedings of the IEEE conference on computer vision and pattern recognition*, pages 4566–4575, 2015. 7
- [41] Shufan Wang, Laure Thompson, and Mohit Iyyer. Phrasebert: Improved phrase embeddings from bert with an application to corpus exploration. *arXiv preprint arXiv:2109.06304*, 2021. 2
- [42] Jason Wei, Xuezhi Wang, Dale Schuurmans, Maarten Bosma, Fei Xia, Ed Chi, Quoc V Le, Denny Zhou, et al. Chain-of-thought prompting elicits reasoning in large language models. *Advances in neural information processing systems*, 35:24824–24837, 2022. 5, 1
- [43] Bin Xiao, Haiping Wu, Weijian Xu, Xiyang Dai, Houdong Hu, Yumao Lu, Michael Zeng, Ce Liu, and Lu Yuan. Florence-2: Advancing a unified representation for a variety of vision tasks. In *Proceedings of the IEEE/CVF Conference on Computer Vision and Pattern Recognition*, pages 4818–4829, 2024. 6, 1
- [44] Le Xue, Manli Shu, Anas Awadalla, Jun Wang, An Yan, Senthil Purushwalkam, Honglu Zhou, Viraj Prabhu, Yutong Dai, Michael S Ryoo, et al. xgen-mm (blip-3): A family of open large multimodal models. *arXiv preprint arXiv:2408.08872*, 2024. 1
- [45] Antoine Yang, Antoine Miech, Josef Sivic, Ivan Laptev, and Cordelia Schmid. Zero-shot video question answering via frozen bidirectional language models. *Advances in Neural Information Processing Systems*, 35:124–141, 2022. 3
- [46] Lihe Yang, Bingyi Kang, Zilong Huang, Zhen Zhao, Xiaogang Xu, Jiashi Feng, and Hengshuang Zhao. Depth anything v2. *arXiv preprint arXiv:2406.09414*, 2024. 6, 1
- [47] Xu Yang, Kaihua Tang, Hanwang Zhang, and Jianfei Cai. Auto-encoding scene graphs for image captioning. In *Proceedings of the IEEE/CVF conference on computer vision and pattern recognition*, pages 10685–10694, 2019. 1, 8
- [48] Xu Yang, Jiawei Peng, Zihua Wang, Haiyang Xu, Qinghao Ye, Chenliang Li, Songfang Huang, Fei Huang, Zhangzikang Li, and Yu Zhang. Transforming visual scene graphs to image captions. *arXiv preprint arXiv:2305.02177*, 2023. 1, 7
- [49] Ting Yao, Yingwei Pan, Yehao Li, and Tao Mei. Exploring visual relationship for image captioning. In *Proceedings of the European conference on computer vision (ECCV)*, pages 684–699, 2018. 8

- [50] Jing Yu, Yuan Chai, Yujing Wang, Yue Hu, and Qi Wu. Cogtree: Cognition tree loss for unbiased scene graph generation. *arXiv preprint arXiv:2009.07526*, 2020. 3
- [51] Qifan Yu, Juncheng Li, Yu Wu, Siliang Tang, Wei Ji, and Yueting Zhuang. Visually-prompted language model for fine-grained scene graph generation in an open world. *arXiv preprint arXiv:2303.13233*, 2023. 2, 3, 7
- [52] Guangyao Zhai, Evin Pinar Örnek, Shun-Cheng Wu, Yan Di, Federico Tombari, Nassir Navab, and Benjamin Busam. Commonsences: Generating commonsense 3d indoor scenes with scene graphs. *Advances in Neural Information Processing Systems*, 36, 2024. 1
- [53] Guangyao Zhai, Evin Pinar Örnek, Dave Zhenyu Chen, Ruotong Liao, Yan Di, Nassir Navab, Federico Tombari, and Benjamin Busam. Echoscene: Indoor scene generation via information echo over scene graph diffusion. In *European Conference on Computer Vision*, pages 167–184. Springer, 2025. 1
- [54] Xiaohua Zhai, Basil Mustafa, Alexander Kolesnikov, and Lucas Bayer. Sigmoid loss for language image pre-training. In *Proceedings of the IEEE/CVF International Conference on Computer Vision*, pages 11975–11986, 2023. 6
- [55] Hongxin Zhang, Weihua Du, Jiaming Shan, Qinhong Zhou, Yilun Du, Joshua B Tenenbaum, Tianmin Shu, and Chuang Gan. Building cooperative embodied agents modularly with large language models. *arXiv preprint arXiv:2307.02485*, 2023. 3
- [56] Yong Zhang, Yingwei Pan, Ting Yao, Rui Huang, Tao Mei, and Chang-Wen Chen. Learning to generate language-supervised and open-vocabulary scene graph using pre-trained visual-semantic space. In *Proceedings of the IEEE/CVF Conference on Computer Vision and Pattern Recognition*, pages 2915–2924, 2023. 2, 3
- [57] Shu Zhao and Huijuan Xu. Less is more: Toward zero-shot local scene graph generation via foundation models. *arXiv preprint arXiv:2310.01356*, 2023. 3
- [58] Yiwu Zhong, Liwei Wang, Jianshu Chen, Dong Yu, and Yin Li. Comprehensive image captioning via scene graph decomposition. In *Computer Vision—ECCV 2020: 16th European Conference, Glasgow, UK, August 23–28, 2020, Proceedings, Part XIV 16*, pages 211–229. Springer, 2020. 1, 7